

Electrochemical properties of Ni-Mn hydroxide and carbon cryogel composite electrodes for supercapacitors

Deuk Yong Lee^a and Young-Jei Oh^{b,c,*}

^aDepartment of Biomedical Engineering, Daelim University, Anyang 13916, Korea

^bOpto-electronic Materials & Devices Research Center, Korea Institute of Science and Technology, Seoul 02792, Korea

^cDepartment of Nano Material Science and Engineering, Korea University of Science and Technology, Daejeon 34113, Korea

The Ni-Mn hydroxide/carbon cryogel (20 to 80 wt%) composite electrodes were synthesized by freeze-drying to improve electrochemical properties of the Ni-Mn hydroxide. XRD results revealed that the composite electrode showed a distorted spinel-like structure similar to the Ni-Mn hydroxide plus the graphitized carbon. The crystallinity of carbon cryogel in composite electrode was improved dramatically with increasing the carbon cryogel content. The presence of the carbon cryogel played a significant role in inhibiting the crystal growth of Ni-Mn hydroxide on the surface of carbon cryogel. Electrochemical properties of the composite electrodes, such as capacitance, power density, and energy density, were observed to be always higher than those of the Ni-Mn electrodes. The highest specific capacitance of 221 F/g was observed for the electrodes containing 20 wt% of carbon cryogel at a scan rate of 5 mV/s and an electrode loading amount of 15 mg/cm² due to easy transport of the ions into pores. However, the highest energy density of 10.8 Wh/kg and power density of 927 W/kg were observed for the composite electrodes containing 80 wt% of carbon cryogel. Experimental results suggested that tunable electrochemical properties of the composite electrodes can be adjusted by varying the carbon cryogel content.

Key words: Ni-Mn hydroxide, Carbon cryogel, Capacitance, Power density, Energy density, Supercapacitor.

Introduction

Lithium secondary battery and electrochemical supercapacitor can be used as a portable power source as an energy storage system using electrochemical principle [1-7]. Although the secondary battery has excellent energy density (the amount of energy that can be accumulated per unit weight or volume), there is still room for improvement in terms of usage time, charging time, and amount of energy available. Although the electrochemical supercapacitor has a smaller energy density than the secondary battery, it exhibits superior characteristics to the secondary battery in terms of use time, charging time, and output density [6]. Manganese and nickel electrode materials display considerable electrochemical activity not only in low discharge rates applied in conventional secondary batteries but also under the usual harsh conditions for the electrochemical supercapacitors [8-11]. Ni-Mn oxide and hydroxide-based electrodes reveal a significant reversible electrochemical activity in the alkaline electrolytes and an extended operating voltage window (~1.8 V) [8]. Ni-Mn ilmenite-based electrode materials demonstrate a low fade rate and high specific electrochemical capacity values at

high discharge rates (up to 70 mAh/g at $I = 70 \text{ mA/cm}^2$) that makes feasible their application in high rate batteries and electrochemical supercapacitors. These metal oxides are widely used as active electrode with polypyrrole, polyaniline, and polythiophene for supercapacitors due to the availability of dual metal cations [8, 12-16]. Carbon-based materials such as activated carbon, carbon black, carbon aerogels, graphene, carbon fiber materials, porous nanocarbon, carbon nanotubes, and multiwalled carbon nanotubes have been widely used in the electrode materials for supercapacitors [6, 12-20]. Carbon aerogels are considered as a promising candidate material for the application of supercapacitors because of high porosity, low electrical resistivity, and high surface area [6]. However, the cost of supercritical drying limits a widespread use. Nowadays, carbon cryogels are emerging as the material of choice for the electrode materials of supercapacitors due to the simplicity because the use of activated carbon or carbon nanotube mixed with the metal oxide powder and the polymer binder may cause the complexity of the process and the deterioration of the electrical conductivity [1-7, 12-20].

The purpose of this study is to solve the problems of the complexity of the process and the deterioration of the electrical conductivity of the composite electrode as a result of the use of the mixed carbon with the metal oxide powder and the polymer binder. In order to improve the power density, the energy density, and the

*Corresponding author:
Tel : +82-2-958-5553
Fax: +82-2-958-5554
E-mail: youngjei@kist.re.kr

capacitance of electrochemical capacitors, we have studied electrodes by adding the freeze-dried carbon cryogel, which has excellent specific surface area and electrical conductivity, to the coprecipitated Ni-Mn hydroxide possessing high specific capacitance and energy density. Carbon cryogels are synthesized by sol-gel polycondensation of resorcinol with formaldehyde, followed by a freeze drying and subsequent pyrolysis in an inert atmosphere [1-7]. Electrochemical properties of the carbon cryogel electrode mixed with Ni-Mn metal oxide are then evaluated.

Experimental

Carbon cryogel

Carbon cryogel possessing a large specific surface area and pore size was prepared to compensate for the drawbacks (low specific surface area and electrical conductivity) of Ni-Mn hydroxide, which is shown in Fig. 1. The aqueous polycondensation of resorcinol (R) with formaldehyde (F) were prepared from resorcinol (Sigma-Aldrich), formaldehyde (Sigma-Aldrich, 37 wt% solution in water), sodium carbonate (Na_2CO_3 , Sigma-Aldrich), and distilled water. After stirring for 1 h, the solution was gelled by curing for 4 days at 50°C . This gel was washed by immersing the gel in *t*-butanol for 1 day. The as-washed gels were frozen for 1 h at -30°C and then dried for 3 days to obtain the RF cryogel [6, 21, 22]. After aging the RF cryogel for 4 h at 250°C , carbon cryogel was prepared by pyrolysis of the cryogel for 4 h at $1,000^\circ\text{C}$, as depicted in Fig. 1. Details of the experimental process is described elsewhere [6].

Ni-Mn hydroxide/carbon cryogel composite electrode

The composite electrode was prepared by mixing Ni-Mn aqueous solution and carbon cryogel (0~80 wt%), as displayed in Fig. 2. Ni-Mn hydroxides were coprecipitated from aqueous solutions followed by freeze drying. The freeze-dried powders were isothermally processed for

2 h at 400°C . The electrode paste was prepared by mixing them with polytetrafluoroethylene (PTFE) binder. The paste was pressed into the nickel foam substrate and then dried for 12 h at 100°C [6, 8].

Electrochemical properties

The electrochemical properties of the composite electrodes were examined at room temperature with a three-electrode apparatus consisting of a working electrode, a Pt counter electrode, and an Hg/HgO reference electrode in KOH solution with different concentrations [6]. Electrochemical properties of carbon cryogel as electrode material in supercapacitor was evaluated using cyclic voltammetry (CV), a galvanostatic charge-discharge test, and electrochemical impedance spectroscopy (EIS). The CV measurements were performed at various scan rates in the range of 5 mV/s and 50 mV/s. Galvanostatic charge-discharge behavior was performed under various constant current densities

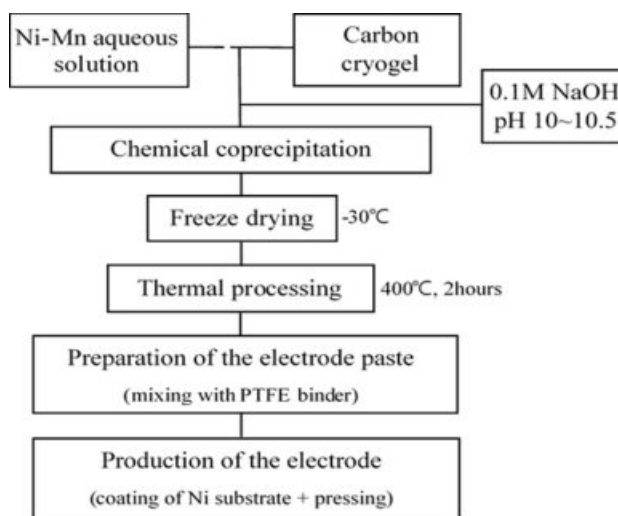


Fig. 2. Manufacturing procedure of Ni-Mn hydroxide+carbon cryogel composite electrode.

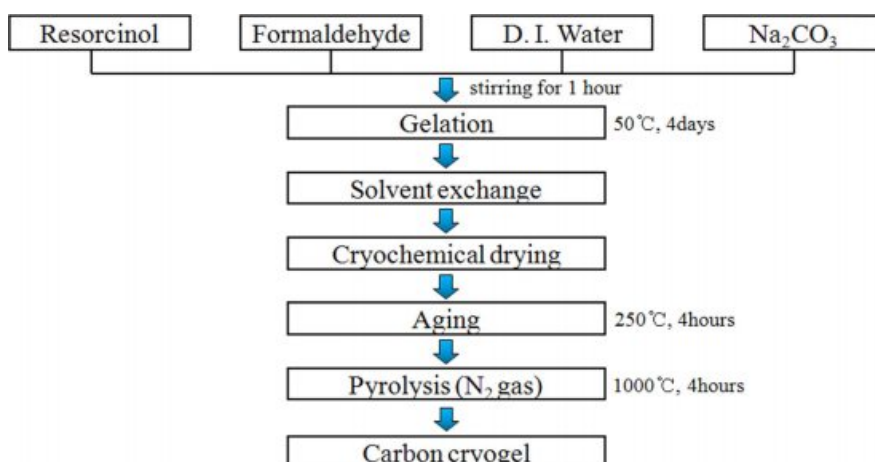


Fig. 1. Fabrication procedure of carbon cryogel.

in a potential between 0 and 1.0 V. Impedance analysis was done with 10 mV amplitude in the frequency range of 100 kHz to 10 mHz using a two-electrode system [13]. Prior to the experiment, carbon cryogel electrodes were immersed in electrolyte for 24 h to diffuse the aqueous electrolyte solution into the pores of carbon cryogel [6, 8, 14-20].

Results and Discussion

Our previous studies revealed that carbon cryogels had a high surface area of 1264 m²/g, large mesopore volumes of 0.63 cm³/g, and average pore diameter of 20 Å [6]. XRD peaks of the carbon cryogels were reported to be located at 2θ of 23.5° and 43.8°, exhibiting the strong (002) and weak (101) diffraction lines, respectively, implying that the carbon cryogels were composed of most amorphous and small amount of graphitized carbons [6]. In the present study, the effect of the amount of carbon cryogel on the electrochemical properties of Ni-Mn and carbon cryogel composite electrodes was investigated. Fig. 3 exhibited that the

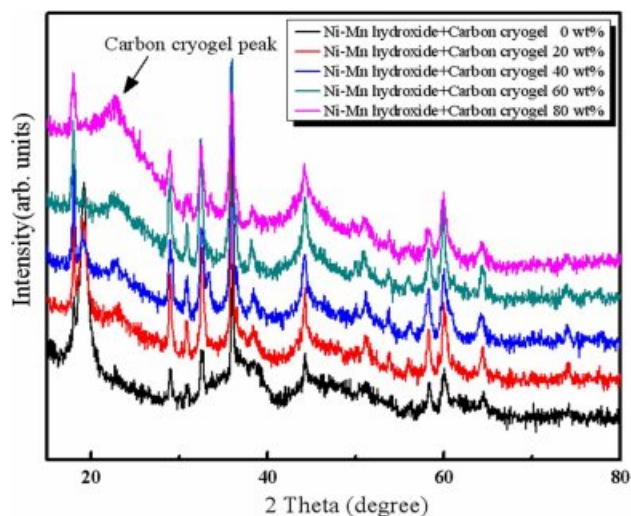


Fig. 3. XRD patterns of Ni-Mn hydroxide and carbon cryogel composite electrodes.

composite electrode showed a distorted spinel-like structure similar to the Ni-Mn hydroxide plus the

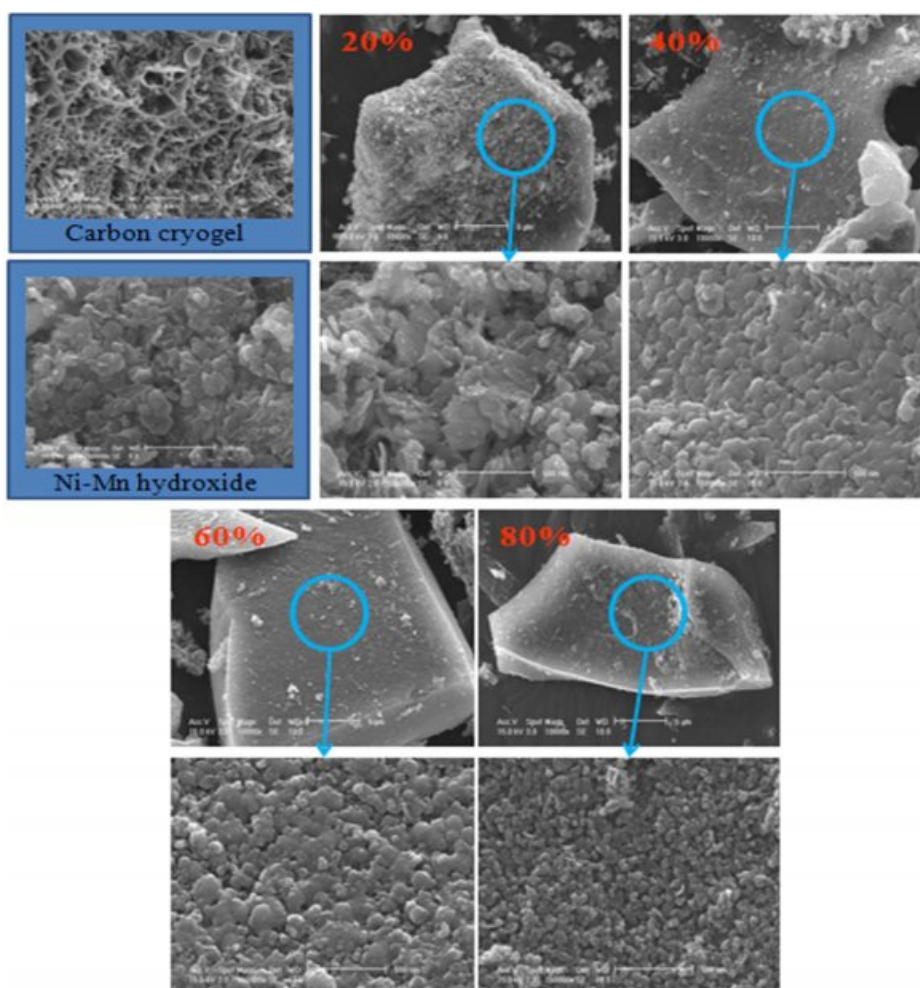


Fig. 4. SEM images of the surfaces of Ni-Mn hydroxide and carbon cryogel composite electrodes. Note that the particle size decreased with increasing the content of carbon cryogel from 20 wt% to 80 wt%.

amount of carbon cryogel increased from 0 to 80 wt%, the peak intensity of graphitized carbon rose dramatically without any second phases, implying that the carbon cryogel can be regarded as graphitized carbon rather than carbon. In addition, the XRD peak of Ni-Mn was slightly shifted to lower angle due to the formation of distorted spinel-like structure [13].

Microstructure of the composite electrode as a function of carbon cryogel concentration was examined as shown in Fig. 4. As the carbon cryogel concentration increased, Ni-Mn hydroxides were uniformly distributed on the surface of carbon cryogel having higher specific surface area. And the particle size of Ni-Mn hydroxide on the surface of carbon cryogel decreased dramatically with increasing the content of carbon cryogel from 20% to 80%. Although physical mechanisms involved are not yet completely understood, the presence of the carbon cryogel played a significant role in inhibiting the crystal growth of Ni-Mn hydroxide.

The CV curves were examined in 6M KOH electrolyte to investigate the variation of capacitance with various scan rates in the range of 5 mV/s to 50 mV/s, as shown depicted in Fig. 5. The specific capacitances of the electrodes (C), as summarized in Table 1, were estimated

from the equation of $C = \{(I_a + |I_c|) / 2W(dV/dt)\}$, where I_a , I_c , W , and dV/dt are the current of anodic and cathodic voltammetric curves on positive and negative sweeps, mass of the composite, and the sweep rate, respectively [6, 23]. As can be seen in Fig. 5 and Table 1, the capacitance started to decrease with increasing the scan rate from 5 mV/s to 50 mV/s. Excellent capacitances were observed for the composite electrode containing 20 wt% of carbon cryogel when the scan rates were in the range of 5 mV/s and 20 mV/s. As the carbon cryogel concentration rose from 20 wt% to 80 wt%, the capacitance decreased from 221 F/g to 181 F/g

Table 1. Capacitance of the Ni-Mn hydroxide and carbon cryogel composite electrodes with various scan rates in 6 M KOH electrolyte.

Carbon cryogel content (wt%)	Capacitance (F/g)			
	5 mV/s	10 mV/s	20 mV/s	50 mV/s
0	195	153	131	81
20	221	194	173	117
40	199	171	157	117
60	196	173	163	131
80	181	161	154	125

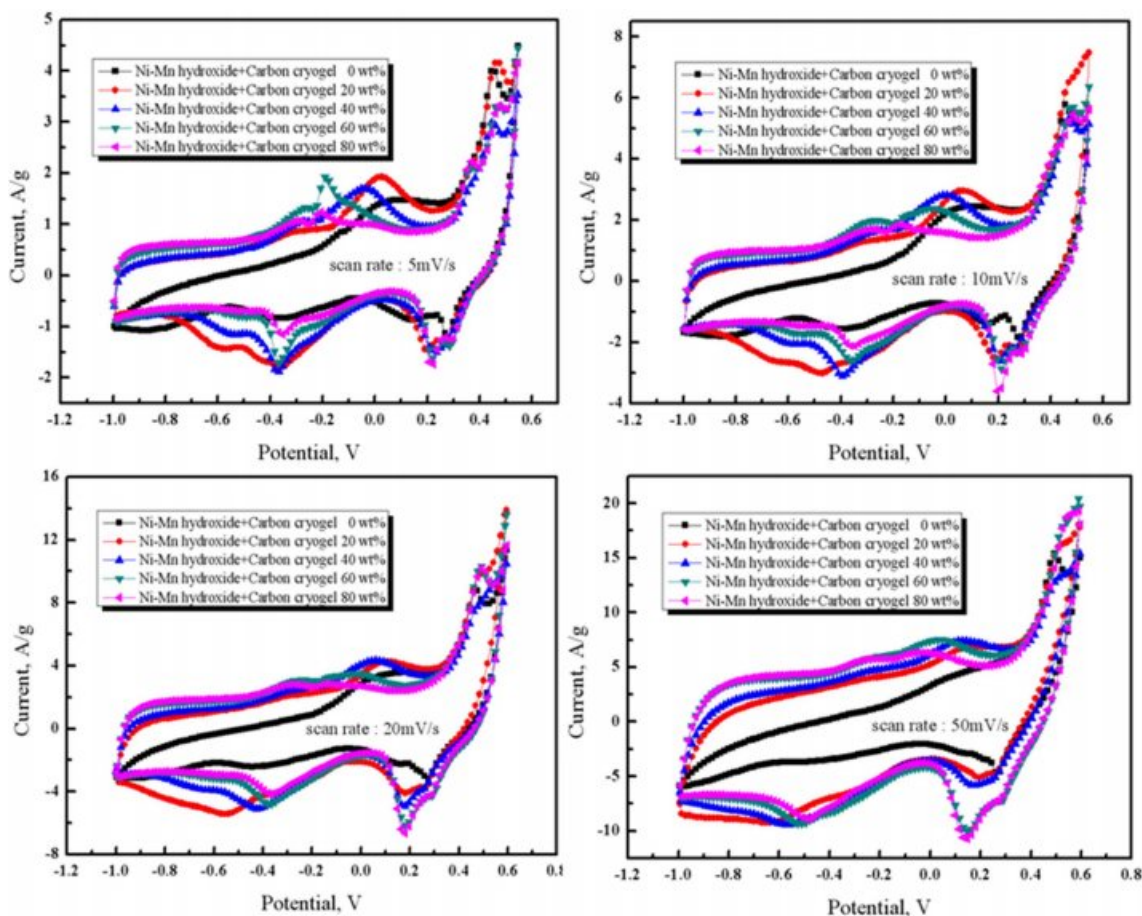


Fig. 5. Cyclic voltammogram of the Ni-Mn hydroxide and carbon cryogel composite electrodes with various scan rates in 6M KOH electrolyte.

g due to the decrease in the amount of Ni-Mn hydroxide. In addition, the specific capacitance of the composite electrode containing 20 wt% of carbon cryogel decreased from 221 F/g to 117 F/g with increasing the scan rate from 5 mV/s to 50 mV/s. It is reported that the ions can transport into pores more easily at low scan rate, however, they had a difficulty in diffusing into pores when scan rates were above 5 mV/s [6]. It is conceivable that the low scan rate (5 mV/s) and the content of carbon cryogel (20 wt%) are mainly attributed to higher capacitance of the composite electrodes.

The imaginary part of the impedance is plotted as a function of real part to compose the impedance spectrum (Nyquist plot), as displayed in Fig. 6. The capacitance can be calculated from the imaginary part of the impedance spectrum according to the equation of $Z'' = 1/2\pi fC$, where f and Z'' are the applied frequency and the imaginary impedance, respectively [6, 12-20]. Electrochemical impedance spectroscopy of the composite electrodes in 6 M KOH electrolyte with different concentrations of carbon cryogel in the range of 0 to 80 wt% revealed that the variation in carbon cryogel concentration can be found in the impedance plot of the composite electrodes. This phenomenon can be evaluated by an equivalent circuit model (Fig. 6). R_1 is the electrolyte resistance. R_2 , R_3 , and Q_2 , represent the contact resistance, the reaction resistance, and the capacitance between carbon cryogel and Ni-Mn hydroxide particles, respectively. C_3 and W_3 are the capacitance of double layer on the surface and the Warburg impedance, respectively [13]. R_1 decreased gradually with increasing the content of carbon cryogel probably due to the use of carbon aerogel and Ni-Mn oxide instead of activated carbon, as displayed in Fig. 6. In the low frequency region, the impedance plot of these capacitors increases, implying that it is purely capacitive. The intersection with the real axis and the first semicircle indicates the internal resistance of the capacitor, which is an equivalent

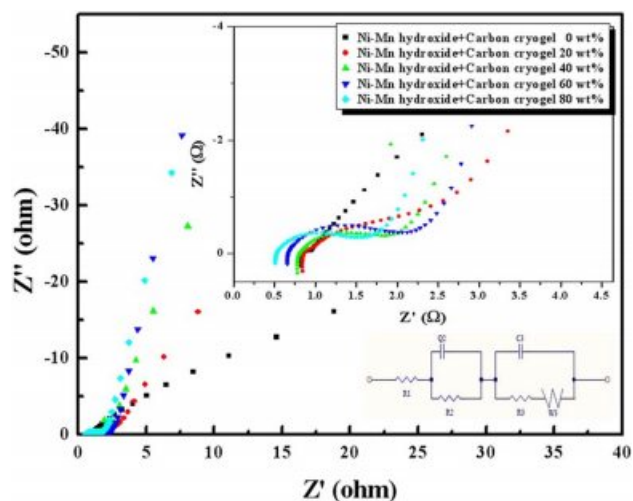


Fig. 6. Electrochemical impedance spectroscopy of carbon cryogel electrode in KOH electrolyte with different carbon cryogel concentration.

series resistance (ESR) of the electrolyte in contact with the current collector and composite electrode. The higher the content of carbon cryogel, the lower the ESR. The combination of resistive and capacitive behaviors of the ions penetrating into the electrode pores leads to a Warburg diffusion line and a capacitive line. The stiffer slope in Fig. 6 implies that the ions can be penetrated into the pores of the composite electrodes more easily with increasing the content of carbon cryogel.

The charge-discharge curves and Ragone plot of the composite electrodes measured in 6 M KOH at current density of 10 mA/cm² are shown in Fig. 7(a). As the carbon cryogel concentration increases, the IR drop occurring at the initial state of discharge decreases and the discharge time becomes longer, suggesting that it can store more energy. The carbon cryogel content is mainly

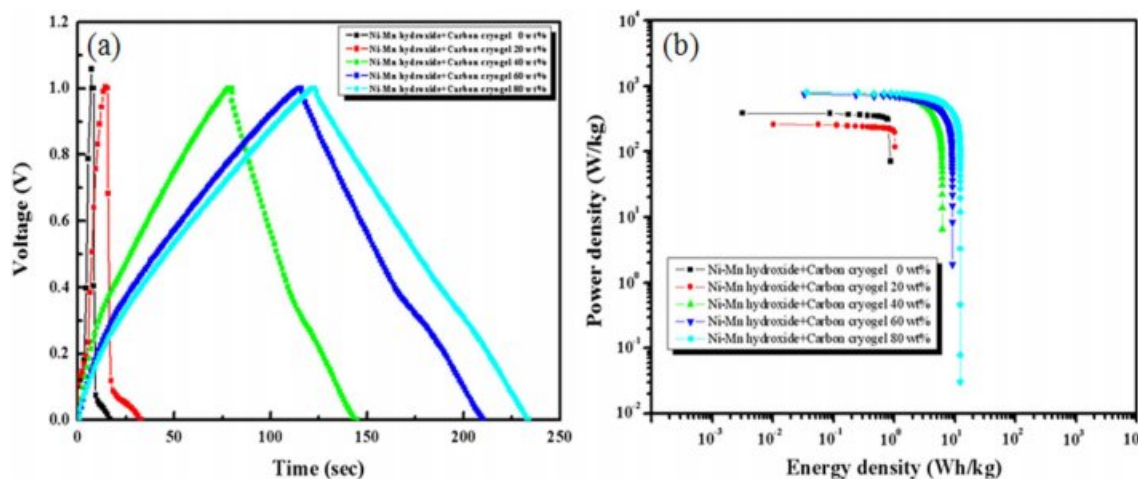


Fig. 7. (a) Charge-discharge curves and (b) Ragone plot of Ni-Mn hydroxide and carbon cryogel composite electrodes.

Table 2. Capacitance, power density, and energy density of Ni-Mn hydroxide and carbon cryogel composite electrodes.

Materials	Capacitance (F/g, at 5 mV/s)	Power density (W/kg, at 10 mA/cm ²)	Energy density (Wh/kg, at 10 mA/cm ²)
Ni-Mn hydroxide	195	568	1.3
Ni-Mn + 20% carbon cryogel	221	396	1.7
Ni-Mn + 40% carbon cryogel	199	921	8.2
Ni-Mn + 60% carbon cryogel	196	912	9.4
Ni-Mn + 80% carbon cryogel	181	927	10.8

attributed to excellent charge-discharge characteristics and energy density. The energy density rose from 1.7 Wh/kg to 10.8 Wh/kg with increasing the carbon cryogel content from 20 wt% to 80 wt%. The specific capacitance and power density are calculated using the charging/discharging characteristics. As a result of Ragone plot (Fig. 7(b) and Table 2), the power density of the electrodes regardless of the carbon cryogel content reached a plateau and then decreases dramatically at a certain value of energy density. The composite electrodes with 80 wt% of carbon cryogel exhibited much better power output of 927 W/kg. In addition, capacitance, power density, and energy density of the composite electrodes can be tailored through the adjustments of the experimental parameters (the content of carbon cryogel, scan rate, and energy density) for supercapacitors.

Conclusions

To improve electrochemical properties of Ni-Mn hydroxide, 20 to 80 wt% of carbon cryogels with high specific surface area and electrical conductivity were added to Ni-Mn hydroxide electrode. XRD results of the composite electrodes revealed that the composite electrode showed a distorted spinel-like structure similar to the Ni-Mn hydroxide plus the graphitized carbon. The electrolyte resistance (R_1) decreased gradually with increasing the content of carbon cryogel. Although the power density and the energy density of the composite electrodes increased with increasing the carbon cryogel concentration, the highest capacitance was observed for the electrodes containing 20 wt% of carbon cryogel due to the reduction in Ni-Mn hydroxides. The Ni-Mn hydroxide and carbon cryogel materials demonstrated sufficient electrochemical activity and high capacitance of 221 F/g at an electrode loading amount of 15 mg/cm², implying that the composite electrodes are suitable for supercapacitors.

References

- J.R. Miller and P. Simon, *Science* 321[5889] (2008) 651-652.
- G. Wang, L. Zhang, and J. Zhang, *Chem. Soc. Rev.* 41[2] (2012) 797-828.
- A.M. Saleem, V. Desmaris, and P. Enoksson, *J. Nanomater.* 2016 (2016) 1537269.
- O.A. Shlyakhtin, S.H. Choi, Y.S. Yoon, and Y.-J. Oh, *Electrochim. Acta* 50[2-3] (2004) 511-516.
- O.A. Shlyakhtin and Y.-J. Oh, *J. Electroceram.* 23 (2009) 452-461.
- M. Song, S. Nahm, and Y.-J. Oh, *J. Korean. Ceram. Soc.* 45[11] (2008) 662-666.
- N.M. Shinde, J.M. Yun., R. S. Mane, S. Marthur, and K.H. Kim, *J. Korean. Ceram. Soc.* 55[5] (2018) 407-418.
- O.A. Shlyakhtin, A.M. Skundin, Y.S. Yoon, and Y.-J. Oh, *Mater. Lett.* 63[1] (2009) 109-112.
- J. Cao, S. Yuan, H. Yin, Y. Zhu, C. Li, M. Fan, and H. Chen, *J. Sol-gel Sci. Technol.* 85 (2018) 629-637.
- M.-S. Jeong, B.-K. Ju, Y.-J. Oh, and J.-K. Lee, *Korean J. Mater. Res.* 21[6] (2011) 309-313.
- O.A. Shlyakhtin, A.M. Skudin, S.J. Yoon, and Y.-J. Oh, *Mater. Lett.* 63[1] (2009) 109-112.
- J.L. Figueiredo, *J. Sol-gel Sci. Technol.* 89 (2019) 12-20.
- H.S. Min, S. Kim, W.-K. Choi, Y.-J. Oh, and J.K. Lee, *Korean J. Mater. Res.* 19 (2009) 544-549.
- J.Y. Hwang, M. Li, M.F. El-Kady, and R.B. Kaner, *Adv. Funct. Mater.* 27 (2017) 1605745.
- S. Ramesh, D. Vikraman, K. Karuppasamy, H.M. Yadav, A. Sivasamy, H. Kim, J. Kim, and H. Kim, *J. Alloy Comp.* 794 (2019) 186-194.
- J. Theerthagiri, G. Durai, K. Karuppasamy, P. Arunachalam, V. Elakkiya, P. Kuppusami, T. Maiyalagan, and H. Kim, *J. Ind. Eng. Chem.* 67 (2018) 12-27.
- J.Y. Hwang, M.F. El-Kady, Y. Wang, L. Wang, Y. Shao, K. Marsh, J.M. Ko, and R.B. Kaner, *Nano Energy* 18 (2015) 57-70.
- S. Chun, B. Evanko, X. Wang, D. Vonlanthen, X. Ji, G.D. Stucky, and S.W. Boettcher, *Nat. Commun.* 6 (2015) 7818.
- Y. Shao, M.F. El-Kady, J. Sun, Y. Li, Q. Zhang, M. Zhu, H. Wang, B. Dunn, and R.B. Kaner, *Chem. Rev.* 118 (2018) 9233-9280.
- M.F. El-Kady and R.B. Kaner, *ACS Nano* 8 (2014) 8725-8729.
- Y. Kim, S. Son, C. Chun, J. Kim, D.Y. Lee, H.J. Choi, and T. Kim, *Biomed. Eng. Lett.* 6 (2016) 287-295.
- O.A. Shlyakhtin, Y.S. Yoon, S.H. Choi, and Y.-J. Oh, *Electrochim. Acta* 50 (2004) 505-509.
- X. Wang, X. Wang, W. Huang, P.J. Sebastian, and S. Gamboa, *J. Power Sources* 140 (2005) 211-215.